Available online at www.sciencedirect.com

ScienceDirect

Biochimica et Biophysica Acta 1772 (2007) 1199–1210

Biochimica et Biophysica Acta BBA

www.elsevier.com/locate/bbadis

Selenium effectively inhibits ROS-mediated apoptotic neural precursor cell death *in vitro* and *in vivo* in traumatic brain injury

Jee Eun Yeo, Soo Kyung Kang *

Department of Physiology, School of Medicine, Pusan National University, 1-10, Ami-Dong, Seo-Gu, Busan, 602-739, South Korea

Received 13 July 2007; received in revised form 13 September 2007; accepted 13 September 2007
Available online 29 September 2007

Abstract

This study was designed to investigate possible prevention of apoptotic cell death by selenium, an antioxidant, using cultured brain-derived neural progenitor cells (NPCs) and an experimental mouse brain trauma (BT) model. We tested some of the neuroprotective effects of sodium selenite in NPC cells by monitoring thioredoxin reductase (TR) expression, optimum H_2O_2 removal, and consequent inhibition of pro-apoptotic events including cytochrome *c* release and caspase 3 and 9 activation. Analysis of key apoptotic regulators during H_2O_2-induced apoptosis of NPCs showed that selenite blocks the activation of c-jun N-terminal protein kinase (JNK)/P38 mitogen-activated protein kinase (MAPK), and Akt survival protein. Moreover, selenite activates p44/42 MAPK and inhibits the downregulation of Bcl2 in selenite-treated NPC cells. For *in vivo* experiments, the effects of selenite on H_2O_2 neurotoxicity were tested using several biochemical and morphologic markers. Here we show that selenite potentially inhibits H_2O_2-induced apoptosis of NPCs and in traumatic brain injury. This *in vivo* protective function was also associated with inhibition of H_2O_2-induced reactive oxygen species (ROS) generation, cytochrome *c* release and caspase 3 and 9 activation. Our data show that the protective function of selenite through attenuation of secondary pathological events most likely results from its comprehensive effects that block apoptotic cell death, resulting in the maintenance of functional neurons and in inhibition of astrogliosis. The finding that selenite administration prevents secondary pathological events in an animal model of traumatic brain injury, as well as its efficacy, may provide novel drug targets for treating brain trauma.

Keywords: Brain trauma; Hydrogen peroxide; Neuroprotection; Oxidation; Sodium selenite

1. Introduction

Traumatic brain injury not only causes direct mechanical damage to tissue, but also induces biochemical changes that lead to delayed neural cell loss [1]. It has been increasingly recognized that such secondary injury may make substantial contributors to chronic neurological disability [2]. Traumatic brain injury is one of the oxidative injuries that also have been linked causally to a variety of neurodegenerative diseases, including Alzheimer's disease [3], Parkinson's disease [4], and amyotropic lateral sclerosis [5], as well as spinal cord injuries and conditions such as ischemia and excitotoxicity. Oxidative damage is mediated by reactive oxygen species (ROS), which can be generated following cell lysis, oxidative burst (as part of the immune response) [6,7] or the presence of an excess of free transition metals (which can act catalytically to generate free radicals) [8]. ROS can also be generated as a byproduct of normal cellular respiration, primarily associated with mitochondrial electron transport [9]. Cellular defense mechanisms against oxidative damage include enzymatic conversion of ROS to less reactive species, chelation of transition metal catalysts and detoxification of ROS by antioxidants [10]. Imbalances in the production of ROS and the actions of protection mechanisms can lead to cell experiencing excessive direct exposure to ROS, and subsequent free radical-induced damage. These damaging effects are normally kept under control by endogenous antioxidant systems including glutathione, ascorbic acid, and enzymes such as superoxide dismutase, glutathione peroxidase,

* Corresponding author. Tel.: +82 51 240 7961; fax: +82 51 246 6001.
E-mail address: skkang@pusan.ac.kr (S.K. Kang).

0925-4439/$ - see front matter © 2007 Elsevier B.V. All rights reserved.
doi:10.1016/j.bbadis.2007.09.004

and catalase. Oxidative stress occurs when antioxidant systems are overwhelmed by ROS, and the resulting oxidative damage can lead to cell death. Neural stem/progenitor cells (NS/PCs) are very sensitive to increases of ROS and this sensitivity results in cell apoptosis. Oxidative stress-induced apoptosis in NS/PCs has often been observed during NS cell therapy and therapeutic irradiation of brain [11]. These findings suggest that oxidative damage to mitochondria is a critical event in oxidative cell damage, and mitochondrial ROS should be a primary target for drug development [11,12]. A number of proapoptotic and antiapoptotic proteins are present in the mitochondrial membrane. Cytochrome *c*, a component of the respiratory chain, has been identified as a proapoptotic molecule present in the mitochondria [12]. The release of cytochrome *c* from the injured mitochondria was recently shown to activate caspase-3 [13]. Bcl-2 is an antiapoptotic protein, which is predominantly present in mitochondria, and prevents apoptosis induced by various agents [14,15]. Bcl-2 prevents cell death by suppressing oxyradical-mediated membrane damage, stabilizing mitochondrial membrane potential, and preventing the release of cytochrome *c* release [16,17].

Selenite, an essential dietary element for mammals, is known to be present in the active center of glutathione peroxidase (GPx), an antioxidant enzyme that protects membrane lipids and macromolecules from oxidative damage produced by peroxides [18,19]. Selenium is also required for the catalytic activity of mammalian thioredoxin reductase, another important anti-oxidant enzyme [21,22]. In addition, selenium has been shown to protect against methamphetamine-induced neurotoxicity [23]. Moreover, positive clinical responses obtained during therapy with selenium and other antioxidants in neurodegenerative diseases have provided substantial evidence for the important role of free radicals and oxidative stress in pathologic processes [24]. Neuroprotective effects of Se have been reported at an experimental level in both methamphetamine-[23] and 6-hydroxydopamine-induced toxicities, as well as in positive clinical responses during therapy with selenite in neurodegenerative diseases [24]. In a recent report, we described some of the protective effects that selenite exerts on both neurochemical and behavioral markers of H_2O_2-induced neurotoxicity in neural progenitor cells derived from mouse brain. Since these positive actions were related to redox modulation as evidenced by decreased lipid peroxidation, we hypothesized that these protective effects might directly involve the antioxidant properties of selenite, most probably related to thioredoxin reductase (TR) expression, optimum H_2O_2 removal, and a consequent inhibition of pro-apoptotic events such as caspase 3 and 9 activation. The present study was also designed to investigate whether MAPK- and ERK-mediated signaling pathways are involved in the anti-apoptotic effect of selenite and whether selenite modulates Bcl2 and Bax expression during apoptotic cell death *in vitro* and *in vivo*. We also detected the effect of selenite on different markers of neurotoxicity and cell death induced by ROS after traumatic damage in mouse brain *in vivo*. For *in vivo* experiments, the effects of selenite on H_2O_2 neurotoxicity were tested using biochemical and morphologic markers.

2. Materials and methods

2.1. Brain-derived neural progenitor cells culture

For preparation of brain-derived NPCs, 4-week-old mice were killed by decapitation. The region of the subventricle zone was dissected out. After removal of the dura, the tissue was minced, washed in sterile Dulbecco's phosphate-buffered saline and digested in a solution of 0.125% of trypsin, DNase (0.01%, Sigma) in Hank's balanced salt solution for 30 min at 37 °C. The cells were plated at a density of 5×10^5 in 10-cm dishes and cultured in serum-free growth medium, which consists of NB (Neurobasal) medium with B27 supplement (Gibco), bFGF (basic fibroblastic growth factor, 10 ng/ml, Sigma), and EGF (epidermal growth factor, 10 ng/ml, Sigma). For expansion of NPCs, cells were grown as neurospheres in petri dish containing NB/B27 and cytokines supplemented culture media [20]. For this study, we usually use 5 to 6 passage NPC cells.

2.2. Sodium selenite treatment and H_2O_2 exposures

For experiment, brain-derived neural progenitors cells (NPCs) were seeded in 10 cm culture dishes at a density of 5×10^5 and cultured in cytokine-free NB/serum-free B27 supplement (B27 Cat No; 17504-044) media for 8 h in a humidified chamber with 5% CO_2. Cells were then pre-treated with sodium selenic acid (Na_2SeO_3, Sigma) (2 ng/ml) for 8 h followed by H_2O_2 (0.03 μM/ml, Sigma) in serum-free DMEM media for a further 6 h. We analyzed cell viability by Tryphan blue exclusion method after 24 h culture. The optimum concentrations of selenite and H_2O_2 were selected according to the preliminary experiment related to cytotoxicity and survival effect of broad range of each reagent. Dilutions of H_2O_2 were made fresh from a 30% stock solution into DMEM just prior to each experiment. Exposures to H_2O_2 were performed by simple addition of a small volume of H_2O_2 diluted in DMEM at ×100 directly to each well, followed by light agitation. For western blotting, cultures were incubated for the times noted, and then toxicity or biochemical measurements were performed. We observed that the toxicity of H_2O_2 was reduced if the H_2O_2 exposures were not performed within 5 min of dilution. This is likely due to the highly reactive nature of H_2O_2 and its short half-life in dilute solutions.

2.3. Analysis of cell viability

Cell viability was assessed by visual cell counts in conjunction with Tryphan Blue exclusion. In all viability assays, triplicate wells were used for each condition, and each experiment was repeated at least three times. For flowcytometric analysis, cells were cultured in 100-mm dishes at densities that ensured exponential growth at the time of harvest. The harvesting and processing protocols used to detect DNA by flow cytometry with propidium iodide were done. Cells were analyzed with a BD Biosciences FACScan (San Jose, CA). Percentages of cells in the G0/G1, S, and G2/M stages of the cell cycle were determined with a DNA histogram fitting program (MODFIT; Verity Software, Topsham, ME). A minimum of 10^4 events /sample was collected. In all viability assays, triplicate wells were used for each condition, and each experiment was repeated at least three times. Raw data from each experiment were analyzed using analysis of variance with Fisher or *t*-test.

2.4. RNA extraction and reverse transcription polymerase chain reaction (RT-PCR)

For RT-PCR, hydrogen peroxide (0.03 μM/ml)-treated cells (selenium pretreated or untreated cell) was cultured for 1 day and then total cellular RNA was extracted with Trizol (Life Technologies, Frederick, MA), reverse transcribed into first strand cDNA using an oligo-dT primer amplified by 35 cycles (94 °C, 1 min; 55 °C, 1 min; 72 °C, 1 min) of PCR using 20 pM of specific primers. PCR amplification was performed using the primer sets. Duplicate PCR reactions were amplified using primer designed GAPDH as a control for assessing PCR efficiency and for subsequent analysis by 1.5% agarose gel electrophoresis. For labeling of PCR products, we used a Syber green detection kit which was purchased from Applied Biosystems (Foster, CA). Semi-

quantitative RT-PCR was performed using an ABI7700 Prism Sequence Detection System. Primer sequences were designed using Primer Express software (PE-Applied Biosystems, Warrington, UK) using gene sequences obtained from the GeneBank database.

Gene	Forward sequence (5′–3′)	Reverse sequence (3′–5′)
GAPDH	CATGACCACAGTC CATGCCATCACT	TGAGGTCCACCAC CCTGTTGCTGTA
Nestin	AACTGGCACACCT CAAGATGT	TCAAGGGTATTAG GCAAGGGG
GFAP	TCCGCCAAGCCAA GCACGAAG	CATCCCGCATCTC CACAGTCT
MMP1	ACAGTTTCCCTGT GTTTCAC	AGTCACTTTCAGC CCAAATA
MMP2	CCTGATGTCCAGC AAGTAGATGC	TTAAGGTGGTGCA GGTATCTGG
GDNF	ATTTTATTCAAGCC ACCATTA	GATACATCCACAC CCTTTAGC
SDF1	GTCCTCTTGCTGTC CAGCTC	GAAGGGCACAGTT TGGAGTG
Tuj	CCTTTGGACACCT ATTCAGG	GTGAGTGTGTCAG CTGGAAG
GDNF	ATTTTATTCAAGCC ACCATTA	GATACATCCAAGC CACCATTA
Trkβ	TCTATGCCGTGGTG GTGATTGC	GCGTCTTCACAGC CACCAGGAT
EGF	ACCAGACGATGAT GGGACAG	GCCAGCACACACT CATCTAT
VEGF	CCTGGTGGACATC TTCCAGGAGTACC	GAAGCTCATCTCT CCTATGTGCTGGC
FGFR2	GAGGCTGTCTCAG AGCCTGT	CTTGCGGCTGTCC ACTTATC

2.5. TUNEL (TdT-mediated dUTP-X nick end labeling) and caspases assays and quantification

The effect of traumatic damage on the induction of apoptosis brain tissue was determined with the TdT *in situ* apoptosis detector kit (Roche, USA), used according to the manufacturer's specifications. After fixation, injured tissue sections with 4% paraformaldehyde were incubated in TUNEL reaction mixture containing deoxynucleotidyl transferase (TdT) buffer with TdT and biotinylated dUTP, incubated in a humid atmosphere at 37 °C for 90 min, and then washed with PBS. The cells were incubated in TUNEL reaction mixture. And then incubated secondary antibody conjugated with the fluorescent markers. The results were analyzed using a Fluorescence Microscope (Leica Microsystem, PA). TUNEL-positive apoptotic cells in brain lesion site were quantified by counting of positively stained cells. Three digital microscopic images at a magnification of 100× were randomly captured at the areas where the positive cells were abundant around lesion site for each section. The number of positively stained cells in the three images was averaged. The result was expressed as relative cells percentage per view field under the microscope. The size of the view field was 0.075 mm^2. Also, we measured Caspases activities in traumatic brain tissue after 1 week of selenium treatment. For Caspase-3, -8, and -9 activity assays, 10 μg of protein in 50 μl total volume was mixed with 50 μl of equilibrated Caspase-Glo 3/7, 8, or 9 reagents (Promega). After incubating at room temperature for 1 h, luminescence was measured using TD 20/20 Luminometer (Turner Designs, Sunnyvale, CA). Blank values were subtracted and fold-increase in activity was calculated based on activity measured from untreated cells. Each sample was measured in triplicate.

2.6. Measurement of intracellular ROS

Intracellular ROS was evaluated using the fluorescent probe DCFDA (5-(and -6)-carboxy-2′, 7′-dichlorodihydrofluorescein diacetate, Sigma). For visualization by fluorescent microscopy, NPC cells were plated in glass bottom dishes and treated with 0.03 μM H_2O_2, alone or with selenite (2 ng/ml), for 6 h. Cells were then washed and loaded with 10 μM of DCFDA for 30 min at 37 °C, and imaged by fluorescent microscopy (ex/em=495/525 nm). For quantitative assessment of ROS production, brain-derived NPC cells in 96-well plates were washed with HBSS and loaded with 10 μM of DCFDA for 30 min at 37 °C. Cells were washed three times with HBSS and exposed to 100 ìM of *t*BHP (Sigma), alone or with SS-31.

2.7. ATP measurement

The amount of protein was determined using the Protein Assay Kit (Bio-Rad, Hercules, CA, USA) following the manufacturer's instructions. Cells were resuspended in buffer containing 150 mmol/l KCl, 25 mmol/l Tris–HCl; pH 7.6, 2 mmol/l EDTA pH 7.4, 10 mmol/l KPO_4 pH 7.4, 0.1 mmol/l $MgCl_2$ and 0.1% (w/v) BSA at a concentration of 1 mg protein per ml of buffer. ATP synthesis was initiated by the addition of 250 μl of the cell suspension to 750 μl of substrate buffer (10 mmol/l malate, 10 mmol/l pyruvate, 1 mmol/l ADP, 40 μg/ml digitonin, and 0.15 mmol/l adenosine pentaphosphate). Cells were incubated at 37 °C for 10 min. At 0 and 10 min, 50 μl aliquots of the reaction mixture were withdrawn, quenched in 450 μl of boiling 100 mmol/l Tris–HCl, 4 mmol/l EDTA (pH 7.75) for 2 min and further diluted 1/10 in the quenching buffer. The quantity of ATP was measured in a luminometer (Berthold, Detection Systems, Pforzheim, Germany) with the ATP Bioluminescence Assay Kit (Roche Diagnostics, Basel, Switzerland) following the manufacturer's instructions.

2.8. Western blot

For confirmation of differentially expressed proteins after selenite treatment in cultured NPC cells and traumatic injured brain, dissected brain lesion site tissues from three or four injured or normal animals and selenite-treated cells were pooled and homogenized (only tissue) and lysed in 500 μl of lysis buffer (20 Mm Tris–HCl [pH 7.5], 150 mM NaCl, 1 mM EDTA, 1% Triton X-100, 2.5 mM sodium pyrophosphate, 1 mM EGTA, 1 mM glycerophosphate, 1 mM Na_3VO_4, and 1 mM PMSF, Sigma). Lysates were clarified by centrifugation at 15,000×*g* for 10 min and the total protein content was determined by a Bio-Rad (Milan, Italy) protein assay kit. For western blotting, equal amounts (40 μg) of protein extracts in a lysis buffer were subjected to 10% SDS-PAGE analysis and transferred to a nitrocellulose membrane. Anti-GFAP, anti-Nestin (1:500, Sigma), anti-MBP (1;400, Chemicon, USA), pSAPK/JNK (1:1000, Cell Signaling), anti-pERK (1:1000, Cell Signaling), anti-Bcl2 (1:1000, Cell Signaling), anti-Bax (1:1000, Cell Signaling), anti-P38 (1:1000, Cell Signaling), anti-Akt (1:1000, Cell Signaling), anti-cytochrome *c* (1:1000, Cell Signaling), and anti-β-Actin (1;500, Sigma) antibodies were incubated with membranes. Relative band intensities were determined by Quality-one 1-D analysis software (Bio-Rad, USA).

2.9. Brain traumatic injury induction and in vivo experimental design

Adult female ICR mouse weighing 30 g or 5-week-old mice were used in our experiments. Animal care was in compliance with Korean regulations on protection and feeding of animals used for experimental and other scientific purposes. Experimental mice were anesthetized with ketamine (75 mg/kg) and xylazine (10 mg/kg). The animal was placed on a heated pad, and a core body temperature was maintained at 38±0.2 °C. Mouse was transferred to a stereotaxic apparatus in a clean field. A 2- to 5-mm incision was made in the scalp 1.5 mm lateral to the bregma. A burr hole was made in the bone 3 mm lateral to bregma with a dental drill. The drill tip was then positioned to the surface of the exposed dura, and made impact and extended at a depth of 5 mm cortical surface and made hall after cutting several time. To evaluate efficacy of selenite, we treated selenite mixed with matrigel or matrigel only into lesion hall of traumatic brain directly. And then, the incision was closed with interrupted 6-0 silk sutures, anesthesia was terminated, and the animals were monitored carefully for at least 4–5 h after surgery and then daily. For this study, we collected enough tissues those were timely harvested for biochemical examination. To evaluate the effect of sodium selenite on acute phase brain trauma pathophysiology, traumatic mice were sacrified after 1 week of injection and then we analyzed. Usually we use three group of mice (n=15) with brain

trauma by traumatic damage induction. The experimental groups were given selenite mixed with matrigel (Gibco-BRL) ($n=15$) and the control group ($n=10$), vehicle or matrigel only. To evaluate the effect of selenite on acutic pathogenic microenvironment of brain trauma (immediately after injury), the mice with brain trauma received varying concentrations of drugs (0, 10, 30, 50 ng/kg) as treatment. Finally, we determined that the optimum selenite concentration was determined for effective treatment of brain trauma mice.

2.10. Sodium selenite administration

Various concentrations of purified sodium selenite were dissolved in HBSS, mixed according to the manufacturer's instructions with matrigel (Gibco-BRL) (0, 10, 30, 50 ng/kg) and injected directly into the lesion site immediately after injury. The control (vehicle) group received the same volume of HBSS mixed with matrigel only. The mice were randomly assigned into two groups: 25 trauma mice receiving the various concentrations of the drug treatment and 5 trauma mice as control. A total of 30 animals were used in these experiments. Immediately after the brain trauma lesion, either the experimental treatment (selenite mixed with matrigel) or the control treatment (HBSS mixed with matrigel) was injected into the lesion cavity close to the cortex and some of striatum of injured brain. The skin incision was closed with silk sutures.

2.11. Histological analysis

The animals were sacrified under sodium pentobarbital anesthetized (60 mg/kg, ip) and their brain fixed by transcardial perfusion with 0.1 M

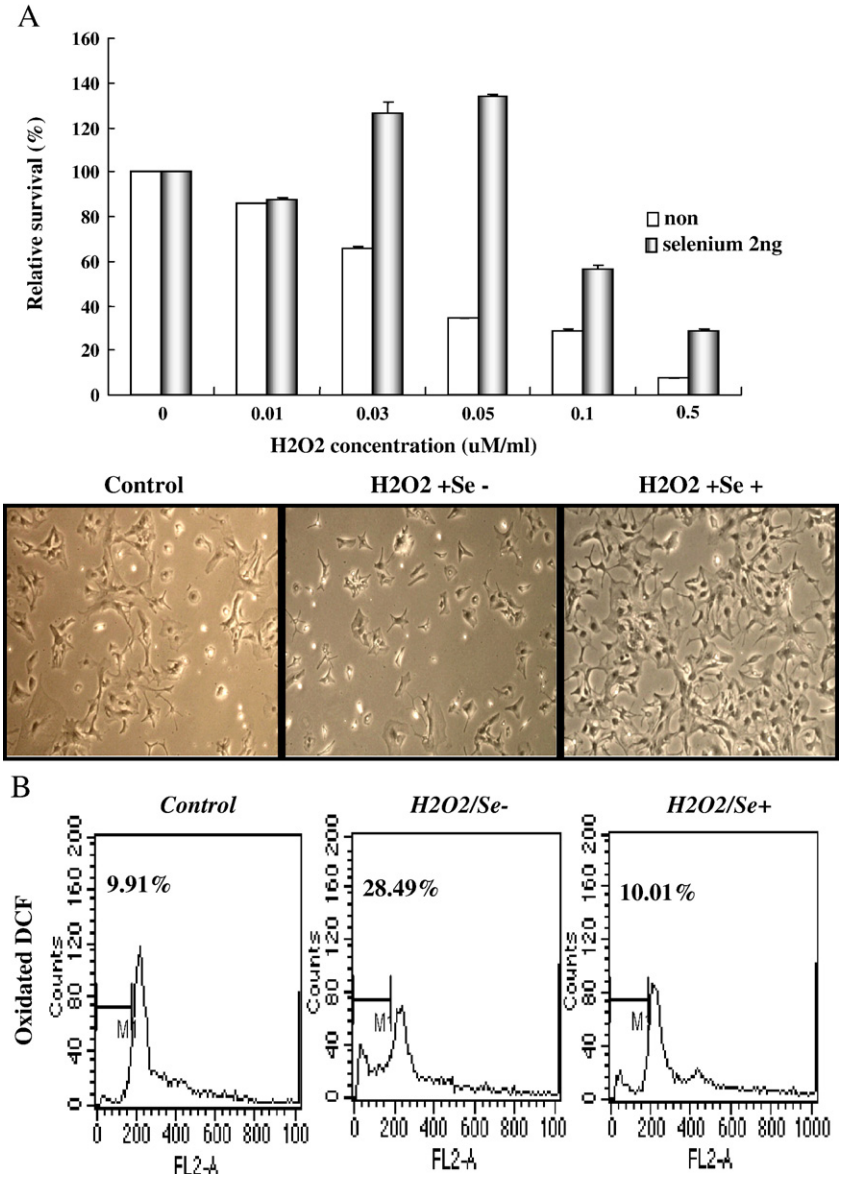

Fig. 1. Effects of sodium selenite on neural progenitor cell survival and growth following H_2O_2-induced apoptotic cell death. (A) Cultured NPCs were treated with several concentrations of H_2O_2 alone or with selenite pretreatment (2 ng/ml). To assess the effect of selenium on cell survival and proliferation, visual cell counts were performed in conjunction with trypan blue exclusion methods. In all viability assays, triplicate wells were used for each condition and each experiment was repeated at least three times. (B) Intracellular ROS was evaluated using the fluorescent probe DCFDA (5-(and-6)-carboxy-2′,7′-dichlorodihydrofluorescein diacetate, Sigma). For visualization by fluorescent microscopy, NPC cells were plated in glass bottom dishes and treated with 0.03 μM H_2O_2, alone or with selenite (2 ng/ml), for 6 h. Cells were then washed and loaded with 10 μM of DCFDA for 30 min at 37 °C, and imaged by fluorescent microscopy (ex/em=495/525 nm). For quantitative assessment of ROS production, brain-derived NPC cells in 96-well plates were washed with HBSS and loaded with 10 μM of DCFDA for 30 min at 37 °C. Cells were washed three times with HBSS and exposed to 100 μM of *t*BHP (Sigma), alone or with SS-31. The oxidation of DCF (5-(and-6)-carboxy-2′, 7′-dichlorodihydrofluorescein) was monitored by fluorescent microscopy.

PBS followed by 4% paraformaldehyde in 0.1 M phosphate buffer. Fixed brain were equilibrated in 30% sucrose for 48 hr and embedded in Tissue-Tek OCT (optimal culture temperature) compound (Miles, Elkhart, IN), and then frozen at −20 °C. Cryostat sections (10 μm) were cut through the brain using a freezing microtome (CM3050; Leika Microsystems), mounted on poly-D-Lysine-coated slides (Sigma); and air-dried overnight at 37 °C. The tissue sections were stained with hematoxylin and eosin (H&E, Sigma) and were examined and photographed with a phase contrast microscope (Nikon Microsystems). For analysis of protein upregulation in injured brain, tissues at the center of the lesion were incubated with overnight at 4 °C with primary antibodies against anti-ED-1 (1:100, Serotec. UK), anti-TuJ (1:250, Sigma, USA), and anti-GFAP (1:2000, DAKO Cytomation, Denmark). After extensive washing with PBS, the tissue sections were incubated for 30 min with FITC and Texas-Red secondary antibodies (1:250, Molecular Probe, USA). Cell nuclei were labeled with Topro-3 (Molecular Probe, USA). The results were analyzed using a Confocal Microscopy (Leica Microsystems, PA) using a Leica TCS sp2 laser scanning microscope equipped with 3 lasers. Immunohistochemical experiments were repeated at least three times. Immuno-positive cells in nearby lesion site (cortex and hippocampus) were quantified by counting of stained cells. Three digital microscopic images at a magnification of 100× were randomly captured at the areas where the positive cells. The number of positively stained cells in the three images was averaged. Three sections at each of the tissue samples were examined by an observer blind to the treatment and the mean value of cell counting was used to represent one single tissue sample. The result was expressed as relative cells percentage per view field. The size of the view field was 0.075 mm^2. Traumatic brain nerve cells staining were performed using 0.25% of Cresyl Echt Violet (Sigma). Cresyl Echt Violet Staining was performed with serial 10 μm tissue slide of brain (4-week post-injury or HBSS injected) and selenite treated were fixed in 95% ethanol, 0.5% acetic acid for 1 h. For each brain tissue slide, samples were harvested at 500 μm intervals to yield 20 sections per brain. Stained sections were viewed on phase contrast microscope. Stained sections around the injury lesion were digitally imaged, and the area of Cresyl Echt Violet staining was analyzed.

2.12. Statistical analysis

All data were presented as mean ± S.E.M. from five or more independent experiments. The statistical significance of difference between groups was calculated by using the Student's two-tailed *t*-test.

3. Results

3.1. Sodium selenite protects neural progenitor cells from H_2O_2-induced apoptotic cell death and affected cell growth

H_2O_2-induced cell death was apparent in the 2-day culture of neural progenitor cells, but was not observed in cultures pretreated with 2 ng/ml selenium (Fig. 1A). In cultures pretreated with sodium selenite (2 ng/ml), over 60% of the neural progenitor cells survived against 0.05 μM/ml H_2O_2-induced apoptotic cell death (Fig. 1A). Cultured neural progenitor cells were able to grow in medium containing 2–5 ng/ml selenium before treatment with 0.03 μM and 0.05 μM H_2O_2 (Fig. 1A). Also, the neural progenitor cells grew well from the second to the fifth day, with 2 ng/ml sodium selenite pretreatment being the optimal concentration for optimum cell growth (supplementary Fig. 2). Cell survival requires active inhibition of apoptosis, which is accomplished either by inhibiting cell death through prevention of DNA breakage (Fig. 1B) or through activation of functional survival proteins.

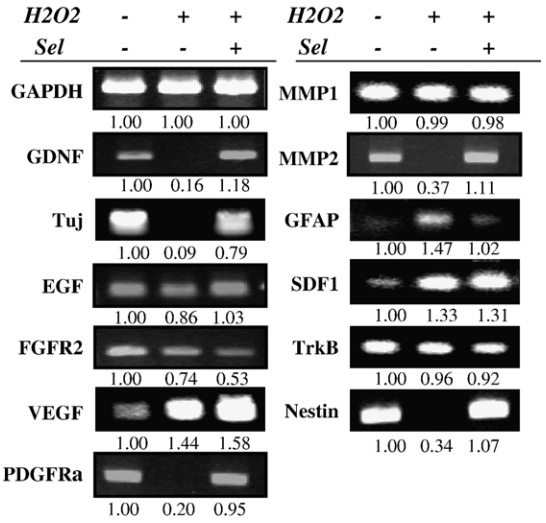

Fig. 2. Effects of selenite on gene expression in NPCs after H_2O_2 treatment. We analyzed functional gene expression in cultured NPCs in the presence or absence of selenium before H_2O_2 treatment; these genes included several kinds of MMPs, SDF1, and stem cell and neural lineage related markers (Nestin, TrkB, FGFR2, GDNF, GFAP and TuJ).

3.2. Effect of selenite on gene expression of neural precursor cells after H_2O_2 treatment

Selenite exerted prominent effects on the expression of various functional genes, including that of several MMPs (matrix metallo-proteases), SDF1 (stem cell migration-related) and stem cell and neural lineage-related markers (Nestin, TrkB, FGFR2, GDNF, GFAP, and TuJ), in neural progenitor cells (NPCs) cultured in the presence or absence of selenium before H_2O_2 treatment. Selenium protected against H_2O_2-induced cytotoxic damage and did not significantly alter the basal levels of GDNF, Nestin, TuJ, MMP2, EGF, and PDGFα mRNA, whereas it decreased the amounts of GFAP, TrkB, SDF1, MMP1, and FGFR2 mRNA at a concentration of 2 ng/ml selenium (Fig. 2). Our results revealed that selenium protected Nestin-positive neural stem cells and TuJ-positive neurons against H_2O_2-induced apoptotic cell death. In contrast, GFAP-positive astrocytes were more sensitive to H_2O_2 and were not protected by selenium pretreatment. According to our preliminary experiments, sodium selenite (2 ng/ml) alone in NPCs had no significant effect on the expression of these genes (data not shown).

3.3. Sodium selenite induced cell survival against H_2O_2-mediated cell death via modulation of P38, p-SAPK/JNK, Bax, Bcl-2 expression in vitro and in vivo

Cell survival requires active inhibition of apoptosis, which is accomplished either by inhibition of cell death through prevention of DNA breakage (Fig. 1B) or by activation of functional survival proteins. When cells were pretreated with selenite, survival and proliferation factors caused the activation and upregulation of p-Akt, p-ERK1/2, Bcl-2, thioreduction reductase 1 (TR1), GFAP, and TuJ proteins in the NSC cultures.

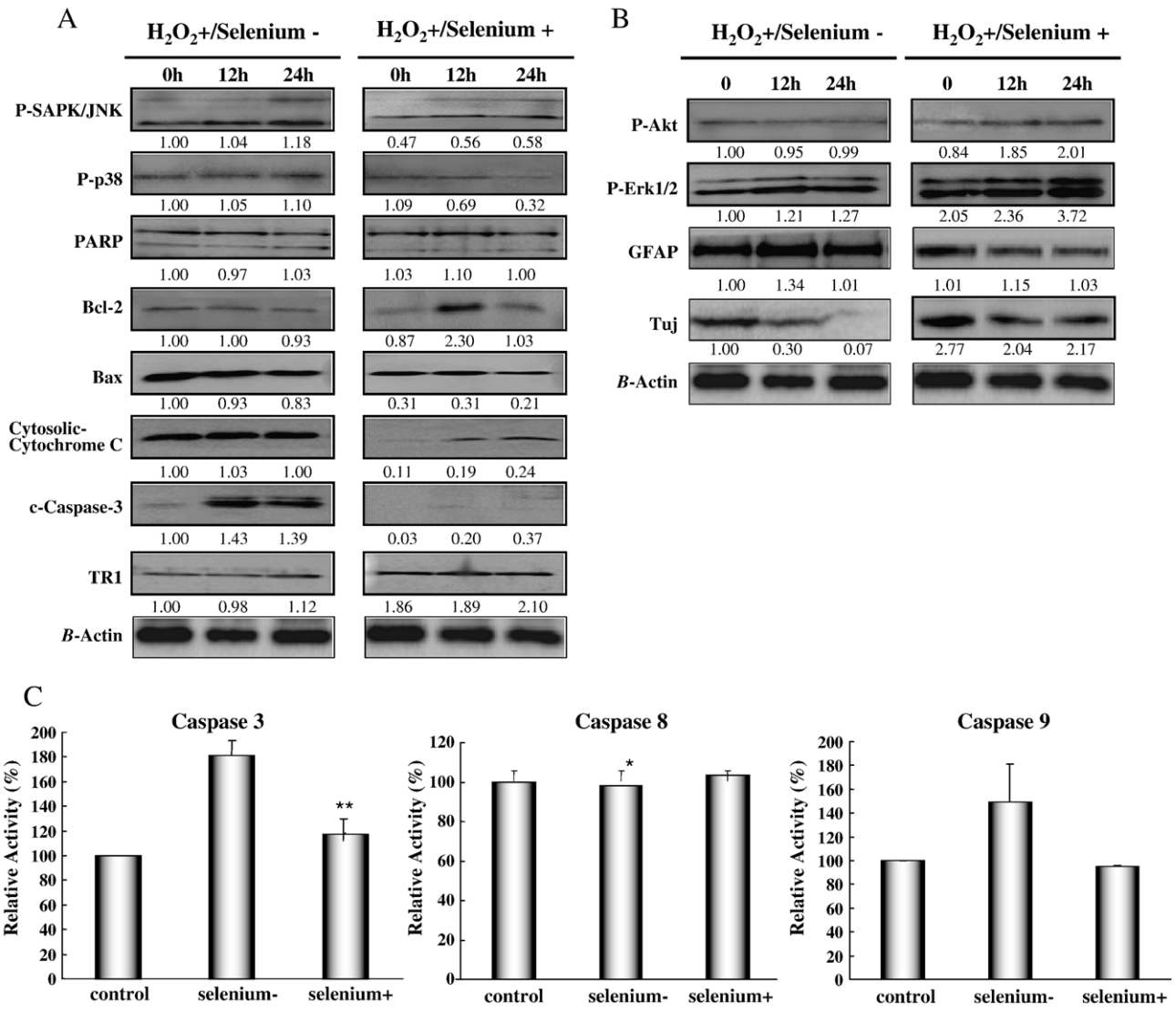

Fig. 3. Effect of selenite on H_2O_2-induced apoptotic/survival signal protein expression in cultured neural progenitor cells. To confirm differential expression of apoptotic or cell survival signal proteins (A) and neural markers (B) in the presence or absence of selenium before H_2O_2 treatment over a time course (0, 12, 24 h), cultured cells were pooled and lysed in 500 μl of lysis buffer. Lysates were clarified by centrifugation at 15,000×*g* for 10 min and the total protein content was determined using a Bio-Rad (Milan, Italy) protein assay kit.

Selenite-treated cells also exhibited attenuated P38, p-SAPK/JNK, Bax, and caspase 3 and 9 (Fig. 3A and C). Selenite-attenuated activation of mitochondria-mediated cell death was related to modulation of caspase 3 and 9 activity, cytochrome *c* release, and PARP cleavage (Fig. 3A and C). To determine the *in vivo* neuroprotective function of sodium selenite, we used a mouse brain traumatic injury model. Traumatic brain injury and H_2O_2 treatment in NPC cells induced P38 and JNK/SAPK activation after 3 days *in vivo* and after 24 h *in vitro* (Figs. 3A, 5A). One week after injury, selenium-treated animals exhibited Bcl2 and thioredoxin reductase (TR1) up-regulation, prominent increases of the neural marker, TuJ, decreased ED1 and GFAP expression (Fig. 5B, C), as well as down-regulation of P38 and p-JNK/SAPK expression after 3 days (Fig. 5A). This result reveals that sodium selenite prominently attenuated the mitochondria-mediated cell death signaling pathway and p38/JNK/SAPK-induced cell death signaling. Finally, selenite negatively regulated neuronal cell death in injured brain tissue and induced neural differentiation. Moreover, sodium selenite attenuated activation of mitochondria-mediated cell death proteins via modulation of caspase 3 and 9 activity and cytochrome *c* release *in vivo* (Fig. 5D and A). Our results suggest that selenite prominently attenuated mitochondria-mediated cell death signaling pathways and protected against neuronal cell death in the injured brain tissue.

3.4. Sodium selenite modulates H_2O_2-induced apoptotic properties in cultured neural progenitor cells

Hydrogen peroxide (H_2O_2) has been shown to increase cellular oxidative stress. We evaluated the effects of selenite on ROS production after treating cultured neural progenitor cells with H_2O_2. Hydrogen peroxide increased the oxidation of DCF in a concentration-dependent manner and the increased DCF

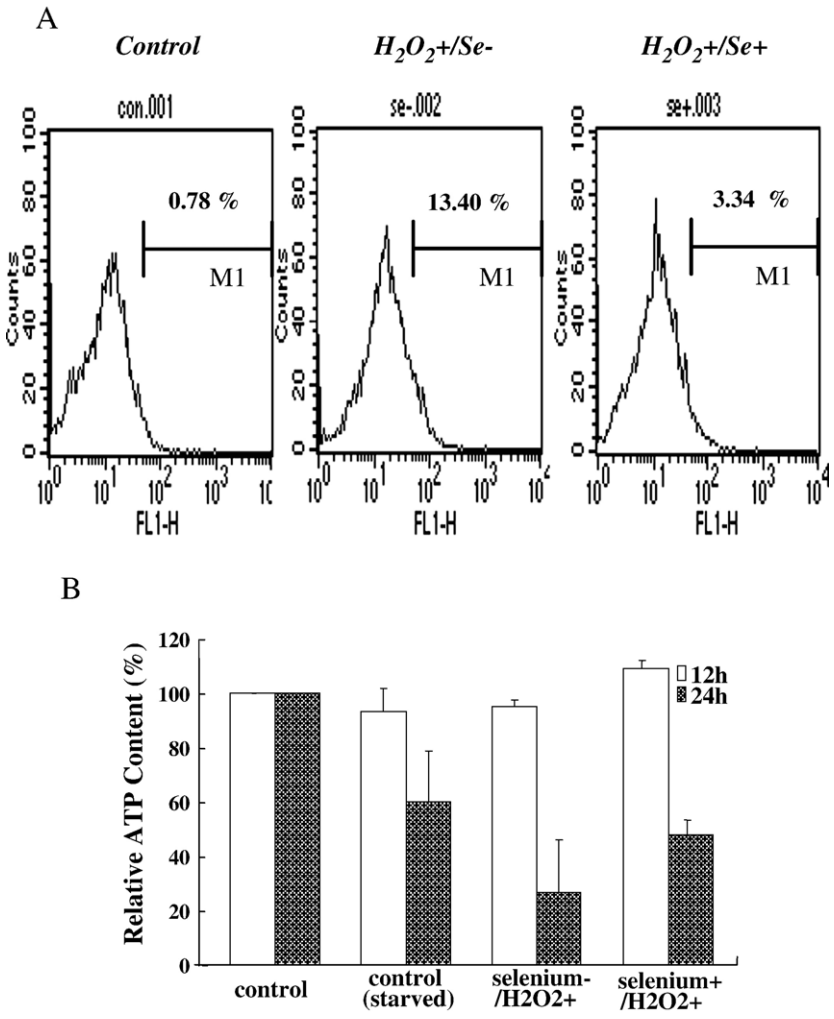

Fig. 4. Effect of selenite on H_2O_2-induced ROS and ATP generation in cultured neural progenitor cells. (A) Intracellular ROS in cultured NPCs was evaluated using the fluorescent probe DCFDA in the presence or absence of selenium before H_2O_2 treatment.

fluorescence intensity was abolished by 2 ng/ml of sodium selenite (Fig. 4A). Selenite alone did not significantly alter ROS production (0.64% ROS generation after selenite treatment in control cells), but selenite decreased H_2O_2-induced ROS production from 13.40% to 3.34% (Fig. 4A). We also examined whether selenite could inhibit the release of cytochrome *c* from mitochondria in selenite-treated cells. Western blot analysis showed that while the H_2O_2-treated cells released most of their cytochrome *c* into the cytosol, cells preincubated with selenite released less of their cytochrome *c* into the cytosol (Fig. 3A), indicating that selenite prevented H_2O_2-induced cell death by maintaining mitochondrial integrity. Because H_2O_2 triggers the activation of caspase 3 and 9, we also examined whether selenite can inhibit caspase 3 and 9 activation after H_2O_2-treatment of NSC cells. In response to H_2O_2 exposure, caspase 3 activity increased by approximately 1.8-fold; selenite treatment significantly attenuated the H_2O_2-elicited caspase activation (Fig. 3C). We also evaluated ATP production in selenite/H_2O_2-treated cells. In response to H_2O_2 exposure, ATP production decreased prominently, but in selenium-pretreated cells, ATP production ability was essentially recovered 24 h after H_2O_2 exposure (Fig. 4B). Together, these findings indicate that selenite inhibits H_2O_2-induced apoptotic features in brain subventricular zone-derived neural progenitor cells.

3.5. Sodium selenite attenuated apoptotic cell death in lesion site of injured brain

Before and after administration of selenite mixed with matrigel into the lesion site, injury-induced cell death was demonstrated by TUNEL staining. As shown in Fig. 6, considerable numbers of TUNEL-positive cells were observed in the lesion site 1 week after traumatic injury. In contrast, selenite treatment effectively prevented the injury-induced TUNEL-positive cells (Fig. 6). Western blot analysis revealed prominently downregulated mitochondria-mediated apoptotic cell death proteins such as cleaved PARP and Bax as well as decreased cytochrome *c* release, with highly increased Bcl2 survival protein in the cytosolic compartment of selenium-treated injured brain compared to untreated brain (Fig. 5A).

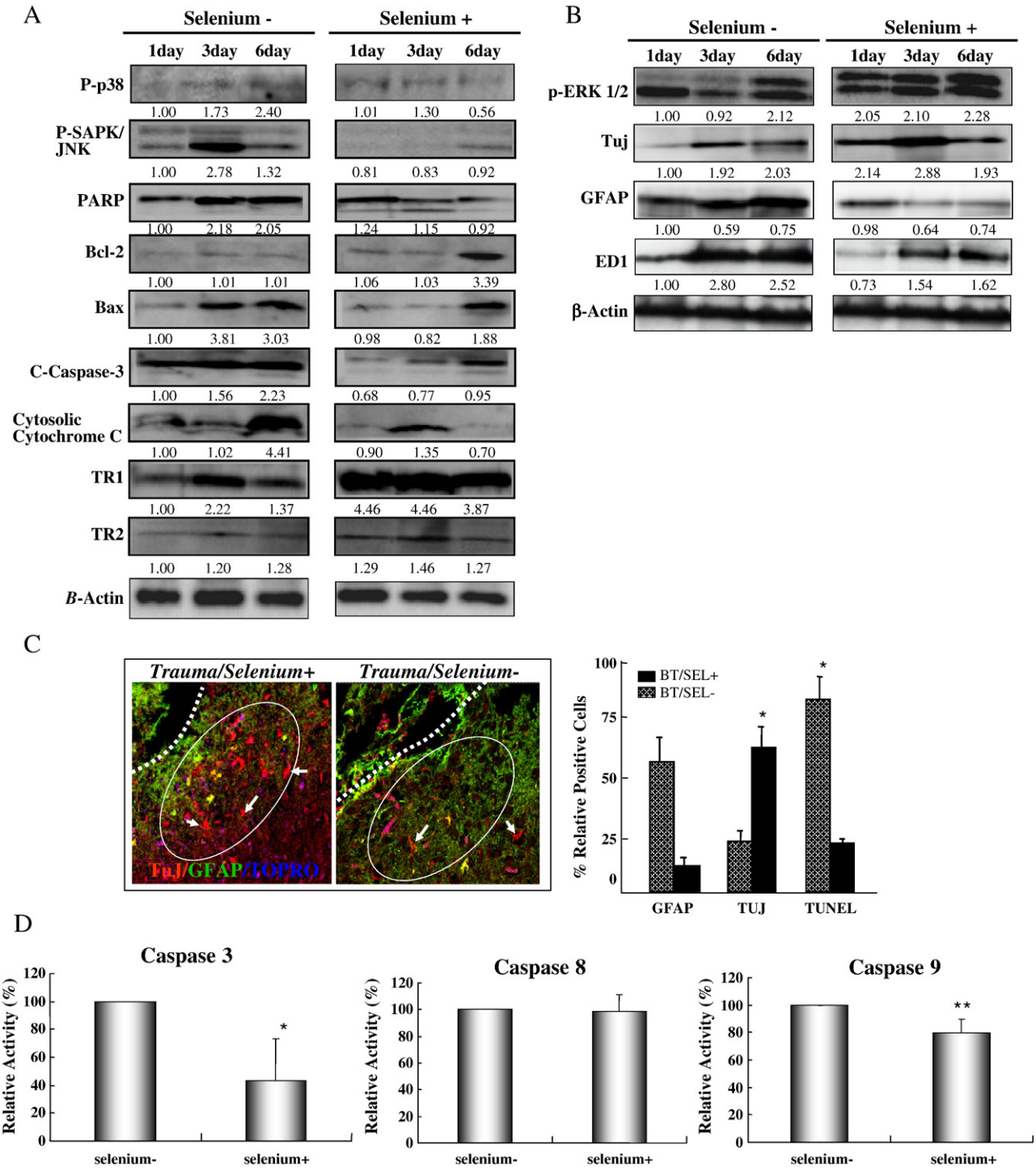

Fig. 5. The neuroprotective function of sodium selenite in traumatic mouse brain injury. (A) Differential expression of the apoptotic signaling proteins at the lesion site after 1 week of sodium selenite treatment in mouse brain. To confirm differential expression of signal proteins and (B) several neural markers after selenite treatment, tissues at the center of the lesion were isolated from the injured brain and analyzed. Relative band intensities were determined using Quality-one 1-D analysis software. (C) To analyze astrogliogenesis and microglia and macrophage activation after selenite treatment in injured brain, tissues at the center of the lesion were incubated with primary antibodies against GFAP and ED. Cell nuclei were labeled with Topro-3. The results are expressed as relative cell percentage per view field. The size of the view field was 0.075 mm^2. The dotted line shows the boundary of the brain lesion site. The circled area indicates the lesion site used to count GFAP- and ED1-positive cells. (D) After 1 week of selenium treatment (or untreated control), we performed caspase activity assays using protein derived from tissue at the lesion site.

Non-injured normal brain tissue sampled from equivalent cortex and striatum regions does not express apoptosis-related signal proteins (data not showed). In addition, compared to the untreated group, the selenium-treated group exhibited prominently preserved TuJ-positive neurons and attenuated glial scar formation (GFAP-positive) (Fig. 5B and C). This result revealed that sodium selenium effectively protected neurons from apoptotic cell death after traumatic brain injury.

3.6. Selenite attenuated injury induced neuron cell death and gliogenesis

To determine whether selenite inhibits posttraumatic astrogliosis, the number of GFAP-positive glia in the two experimental groups were compared. Cortex surrounding the lesions was sliced into 3-μm thick sections and quantitatively examined for GFAP-positive glial cells in the white matter region. There were 3.84 ± 2.0 astroglia per 20 μm^2 of tissue in the selenite-treated group vs. 18.0±1.7 astroglia per 20 μm^2 of tissue in the untreated control group (Fig. 5C). The number of GFAP-immunopositive cells in the ventral funiculi demonstrated an overall significant effect on reducing reactive astrogliosis (Fig. 5B, C). In contrast to the GFAP/TOPRO3-positive population (%), there were significantly more TuJ/TOPRO3-positive neurons (%) around the lesion site (Fig. 5C). Cresyl echt violet staining was performed at the lesion site in the injured brains to detect neurons (Fig. 6). In normal brains and in selenite-treated mice, the violet groups of nerve cells indicated the prevention of neuronal death. In contrast, in the traumatic brain injury control group, cresyl echt violet staining in the same area was very weak. Selenite treatment greatly improved TuJ expression around the lesion site in the selenite/trauma-administered group as an indicator of neuroprotection after insult (Fig. 5B). Selenite treatment also reduced the loss of neurons in the injured cortex and hippocampus. Cresyl echt violet staining in the lesions of control injured brain tissue was completely lost, while the loss was not observed in the normal and selenite-treated animals (Fig. 6). Finally, selenite treatment reduced and attenuated neuron death at the lesion sites. The overall cross section profiles of the lesion epicenters from the normal, control, trauma, and selenite/trauma animals were comparable. We also evaluated whether selenite treatment reduced lesion volume. We outlined the lesion area in transverse sections of brain samples from the lesions and adjacent tissue. The transverse lesion lengths indicated that selenite significantly affected the lesions. The lesions may also have been influenced by the possible neuroprotective properties of selenite. We observed a dose-dependent effect of selenite (0, 10, 30, 50 μg/kg) on the expression of caspase 3, caspase 8, caspase 9, and PARP by staining TUNEL-positive cells at the injury epicenter. At 10 ng/kg, selenite significantly reduced caspases and PARP expression to negligible pre-trauma levels (data not shown).

3.7. Effect of selenite on macrophage and microglia infiltration in traumatic brain injuries in a mouse model

Sham-operated or control brain trauma animals and selenite-treated (10 μg/kg) animals were evaluated 6 days after surgery

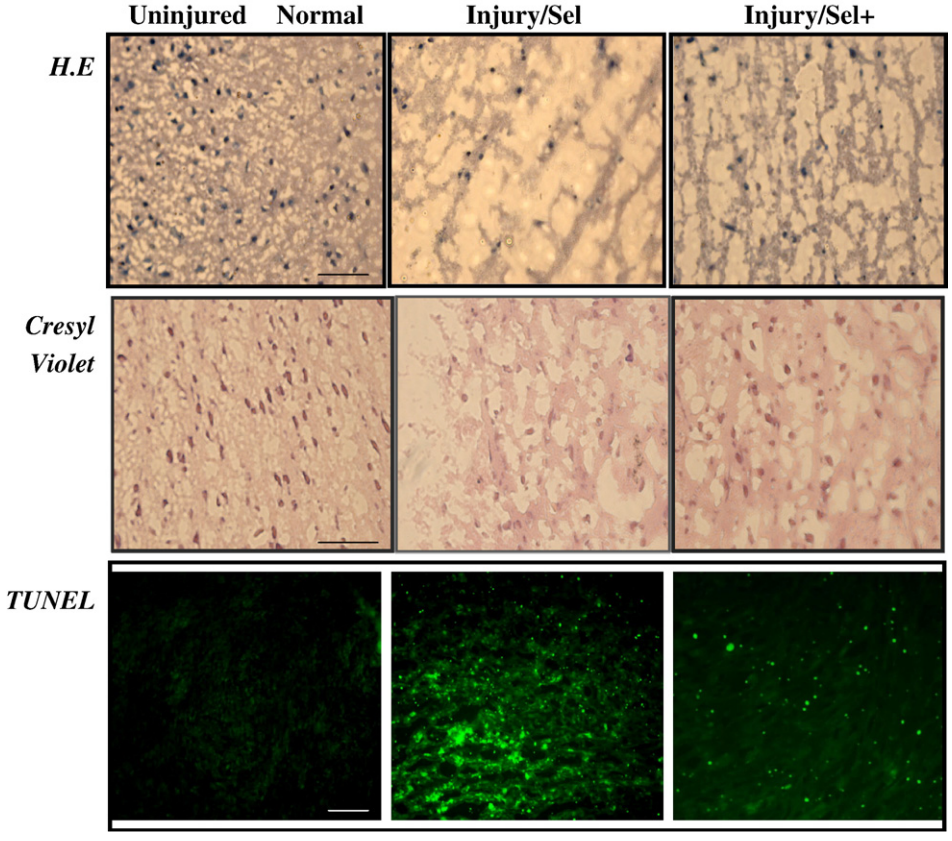

Fig. 6. The effect of sodium selenite on neuroprotection in traumatic brain injury. Sodium selenite attenuated apoptotic cell death after traumatic brain injury. (A) Representative micrographs of the lesion in normal and injured animals following staining with cresyl echt violet and Luxol fast blue, respectively. One week after traumatic brain injury in selenium-treated or untreated tissue, nerve cells were stained with 0.25% cresyl echt violet solution. (B) The effect of selenite on induction of apoptosis by traumatic brain injury was determined with the TdT *in situ* apoptosis detector kit according to the manufacturer's specifications. The results were analyzed using a Fluorescence Microscope (Leica Microsystem, PA). TUNEL-positive apoptotic cells in traumatic brain lesions were quantified by counting positively stained cells.

and treatment. We found prominent differences between the control and experimental groups in the expression of ED-1 protein during the examination period. The expression of ED-1 antigenic protein level decreased remarkably after selenite treatment (Fig. 5B). Indeed, selenite treatment had a direct effect on macrophage invasion. Traumatic injury activated both macrophage and microglia at the lesion sites as indicated by the ED-1 immunohistochemistry, which showed that the number of activated macrophages increased significantly. They were darkly stained with round, sharp and blunt processes in the tissue around the lesion sites 1 week after injury (data not shown).

4. Discussion

Oxidative stress and generation of reactive oxygen species (ROS) are strongly implicated in a number of neuronal and neuromuscular disorders, including stroke, cerebrovascular disease, Alzheimer's disease, Parkinson's disease, familial amyotrophic lateral sclerosis, and Duchenne muscular dystrophy [25–32]. Selenium is known to provide protection from ROS-induced cell damage, and the proposed mechanism mainly invokes the functions of glutathione peroxidases (GPxs) and selenoprotein P (SelP). Selenium/selenite has been linked to regulatory functions in cell growth, survival, and cytotoxicity, as well as transformations possibly involving redox regulation, chemical toxicity and the transcriptional regulation of various genes (Lee et al., 2000). In a recent study, we also found a significant protective effect of sodium selenite against hydrogen peroxide (H_2O_2)-induced NPC death in an *in vitro* culture system (Fig. 1). Selenite-induced protection and survival of NPCs involved continued expression of cell migration and stem cell function-related genes such as MMP2, SDF1, GDNF, PDGFRα, and Nestin after H_2O_2 exposure (Fig. 2). Our RT-PCR results also showed that selenite especially protects Nestin-positive neural precursor cells and TuJ-positive neurons against ROS-mediated apoptotic cell death (Fig. 2). The precise biochemical action of selenite, however, is not yet fully understood. Thioredoxin reductase and thioredoxin form a redox system that has multiple roles, including redox regulation of transcription factors and provision for reducing equivalents for synthesizing deoxyribonucleotides for DNA synthesis. Selenium induces mitochondrial permeability transition by modification of protein thiol groups, which results in cytochrome *c* release and loss of mitochondrial membrane potential [33]. We provide experimental support for the hypothesis that selenite may play a pivotal role in the anti-oxidation responses, in part by significantly inhibiting production of ROS, an important mediator in the pathophysiology of inflammatory disease such as acute brain trauma (Fig. 4A). Activation of both resident and recruited immune cells appears to be the cellular source for up-regulation of these cytokine mRNAs in SCI-induced CNS inflammation [34]. Macrophages play important roles in the removal of myelin debris and the products of neuronal degeneration after trauma, infection, or autoimmune reactions in the neuronal system. Recent evidence [34] indicates that this activation may account for apoptosis induced by proinflammatory cytokines. It is apparent that the inflammatory response to LPS in macrophages includes the initial induction of ROS in macrophages, which leads to activation of MAPKs and NFκB and to the induction of iNOS and inflammatory cytokines. This last step leads to production of toxic amounts of NO, together with toxic cytokines. Selenite can alleviate these effects by antioxidant action and by modulating the downstream pathway. Our results suggest that the selenite-modulated pathway involves Bax and cytochrome *c*, while p38/JNK and PARP-specific ERK showed little involvement in the *in vitro* cultured NPCs and *in vivo* traumatic brain lesion (Figs. 3A, B, 5A, B). The short-term effect of selenite is mainly anti-apoptotic. Cellular damage from ROS was greatly alleviated by selenite treatment. Selenite incubation resulted in lower levels of intracellular ROS and prevention of p38, SAPK-JNK, and Bax activation in *in vitro* cultures (Fig. 3). An important intracellular signal transduction pathway that leads to apoptosis after brain trauma involves activation of MAPKs and caspases. Recent studies with *in vivo* and *in vitro* models of CNS trauma demonstrate that MAPKs are activated in response to mechanical forces. Both c-Jun N-terminal kinase (JNK) and extracellular signal-regulated kinase (ERK 1/2) are known regulators of cell survival/death, and activation of ERK 1/2 was linked to cell survival [35,36]. Activated JNK was evident in both apoptotic neurons and oligodendrocytes following compressive spinal cord injury [37], and delayed neuronal death following global cerebral ischemia was preceded by a sustained increase in activated JNK [38]. In contrast to JNK, activated ERK 1/2 may be involved in the regulation of axonal growth [39], in the protection against cytosine arabinoside-induced apoptosis [40], and in neuroprotection in a model of ischemic preconditioning [41]. Ebselen also reported inhibition of NO-induced apoptosis of differentiated PC12 cells via inhibition of ASK1-p38, MAPK-p53 and JNK signaling and via activation of p44/42MAPK and Bcl2 [42]. Our results show that ERK, P38, and JNK were consistently activated by traumatic brain injury (Fig. 5A). When selenite was used to treat NPCs and *in vivo* traumatic brain injuries, p38 and JNK activation was decreased (Figs. 3A, 5B). After H_2O_2 treatment in NPCs and cortical impact injuries in mice, ERK phosphorylation increased at the lesion sites and in the cells (Fig. 5B). After treating the traumatic brain injuries and the reactive oxygen-damaged cells with selenite, ERK activation increased greatly (Figs. 3B, 5B), suggesting a beneficial role for ERK in functional neural recovery. Furthermore, disrupting the balance between pro- and anti-survival MAP kinases following CNS injury may lead to cell death.

Likewise, Akt is an important signaling mediator of cell survival, metabolism, and cell cycle progression [43,44]. The PI3K/Akt signaling pathway promotes cell survival by phosphorylating and inactivating pro-apoptotic proteins. Activated Akt can also inhibit JNK activity in cells where JNK mediates apoptosis. Akt activation has been observed in cultured NPCs after treatment with H_2O_2. Compared to control, selenium-treated cells exhibited a large increase in the expression of phospho-Akt molecules (Fig. 3B). Highly activated Akt may modulate JNK activities that mediate cell death and ultimately induce an escape from apoptotic cell death.

Caspase activation, which occurs at the site of trauma after brain injury, was also effectively prevented (Fig. 3C). The present study extends these observations to the brain lesion site by providing the first evidence that up-regulation of Bcl2 protein also plays an important role in the execution of apoptosis in brain trauma. Activated caspase-3 protease contributes to the execution of apoptosis. In addition, cleavage of the DNA repair enzyme PARP during apoptosis not only blocks DNA repair, but also preserves cellular pools of ATP that may be necessary for execution of the cell death program. Compared with untreated control brain, the tissue lesions in selenite-treated brains showed significant decreases in the total amount of PARP and Bax apoptotic proteins and in cytochrome *c* released, and increases in the expression of Bcl2, an anti-apoptotic survival protein (Fig. 5A). Selenite effectively blocked ROS-mediated apoptotic cell death (TUNEL-positive) in the lesion site (Fig. 6). The foremost protective effect of selenite in brain trauma would therefore manifest in suppression of acute secondary apoptotic cell death. Indeed, selenite treatment prevented the elevation of ROS generation in cultured NSCs after H_2O_2 treatment and protected against neuronal cell (TuJ-positive) death, which is seen prominently in mouse brain trauma (Fig. 5B and C). Selenite also attenuates active microglia and macrophage infiltration very efficiently (Fig. 5B). This finding supported the prominent histopathological changes, such as attenuation of glial scar formation, observed in the lesion area in selenite-treated mouse brains (Fig. 5C). Moreover, selenite-mediated neuroprotection has been linked to its attenuation of p38 mitogen-activated protein kinase, pSAPK/JNK (Fig. 5A).

Our data show that the therapeutic outcome of selenite treatment most likely resulted from its comprehensive prevention of apoptotic cell death, thus protecting neurons and inhibiting microglial and macrophage cell activation (Figs. 5 and 6). Selenite inhibits the processes of apoptotic cell death at the brain lesion site and is suggested to be responsible for delayed cell death in cortical and hippocampal pathology (Figs. 5 and 6). Selenite significantly attenuated cortical damage and increased neuron survival at the brain lesion sites. Moreover, there was a remarkable reduction in reactive astrogliosis in the lesioned cortex (Fig. 5B and C). Reactive astrocytes secrete inhibitory molecules such as neurocan and trabecular meshwork-inducible glucocorticoid response protein (TIGR) to restrict motor neuronal repair and regeneration [45,46].

The contribution of selenite to the reduction of apoptotic cell death and prevention of neuronal destruction in the cortex and hippocampus following traumatic injury require further study in order to fully elucidate a mechanism. The findings that selenite prevents secondary pathological events in traumatic brain injuries in an animal model may provide novel drug targets for treating brain trauma.

Acknowledgements

This study was supported by the 21st Century Frontier/Stem Cell Research Committee (SC3130) and Korea Science and Engineering Foundation (KOSEF) grant funded by the Korea government (MOST) (M1064145000206N).

Appendix A. Supplementary data

Supplementary data associated with this article can be found, in the online version, at doi:10.1016/j.bbadis.2007.09.004.

References

[1] A.G. Yakovlev, A.I. Farden, Mechanisms of neural cell death: implications for development of neuroprotective treatment strategies, NeuroRX 1 (2004) 5–16.
[2] A.I. Faden, Neuroprotection and traumatic brain injury: theoretical option or realistic proposition, Curr. Opin. Neurol. 15 (2002) 707–712.
[3] S.J. Richardson, Free radical in the generation of Alzheimer's disease, Ann. N.Y. Acad. Sci. 67 (1993) 119–127.
[4] C.W. Olanow, An introduction to the free radical hypothesis in Parkinson's disease, Ann. Neurol. (1992) S2–S9.
[5] C.W. Olanow, A radical hypothesis for neurodegeneration, Trends Neurosci. 16 (1993) 439–444.
[6] P. Bellavite, The superoxide-forming enzymatic system of phagocytes, Free Radic. Biol. Med. 4 (1988) 225–261.
[7] D. Giulian, K. Vaca, M. Corpuz, Brain glia release factors with opposing actions upon neuronal survival, J. Neurosci. 13 (1993) 29–37.
[8] B. Halliwell, J.M. Gutteridge, Biologically relevant metal ion-dependent hydroxyl radical generation :an update, Fedn. Eur. Biochem. Socs. Lett. 307 (1992) 108–112.
[9] C. Richter, G.E. Kass, Oxidative stress in mitochondria: its relationship to cellular Ca2+ homeostasis, cell death, proliferation, and differentiation, Chem. Biol. Interact 77 (1991) 1–23.
[10] B.P. Yu, Cellular defenses against damage from reactive oxygen species, Physiol. Rev. 74 (1994) 139–162.
[11] M.P. Murphy, R.A. Smith, Drug delivery to mitochondria: the key to mitochondrial medicine, Adv. Drug Deliv. Rev. 41 (2000) 235–250.
[12] X. Liu, C.N. Kim, Y. Yang, R. Jem merson, X. Wang, Induction of apoptosis program in cell-free extracts: requirement for dATP and cytochrome *c*, Cell 86 (1996) 145–157.
[13] R.M. Kluck, E. Bossy-Wetzel, D.R. Green, D.D. Newmeywer, The release of cytochrome *c* from mitochondria: a primary site for Bcl-2 regulation of apoptosis, Science 275 (1997) 1132–1136.
[14] N.M. Itoh, Y. Tsujimoto, S. Nagata, Effect of Bcl-2 on Fas antigen-mediated cell death, J. Immunol. 151 (1993) 621–627.
[15] J.C. Reed, Double identity for proteins of the Bcl-2 family, Nature 387 (1997) 773–776.
[16] A.J. Bruce-Keller, J.G. Begley, W. Fu, D.A. Butterfield, D.E. Bredesen, J.B. Hutchins, K. Hensley, M.P. Mattson, Bcl-2 protects isolated plasma and mitochondrial membranes against lipid peroxidation induced by hydrogen peroxide and amyloid B-peptide, J. Neurochem. 70 (1998) 31–39.
[17] S. Desagher, J.C. Martinou, Mitochondria as the central control point of apoptosis, Trends Cell Biol. 10 (2000) 369–377.
[18] J.T. Rotruck, A.L. Pope, H.E. Ganther, A.B. Swanson, D.G. Hafeman, W.G. Hoekstra, Selenium: biochemical role as a component of glutathione peroxidase, Science 179 (1973) 588–590.
[19] D. Arman, Free radicals and age-related diseases, Free Radicals in Aging, 1993, pp. 205–222.
[20] S.K. Kang, S.H. Cha, H.G. Jeon, Curcumin-induced histone hypoacetylation enhances caspase-3-dependent glioma cell death and neurogenesis of neural progenitor cells, Stem Cell. Dev. 15 (2) (2006) 165–174.
[21] L. Marcocci, L. Floche, L. Packer, Evidence for a functional role of the selenocysteine residue in mammalian thioredoxin reductase, Biofactors 6 (1997) 351–358.
[22] S.R. Lee, S. Bar-Noy, J. Kwon, R.L. Levine, T.C. Stadtman, S.G. Rhee, Mammalian thioredoxin reductase: oxidation of the C-terminal cysteine/selenocysteine active site forms a thioselenide, and replacement of selenium with sulfur markedly reduces catalytic activity, Proc. Natl. Acad. Sci. U. S. A. 97 (2000) 2521–2526.
[23] S.Z. Imam, G.D. Newport, F. Islam, W. Slikker, S.F. Jr, Ali, Selenium, an antioxidant, protects against methamphetamine-induced dopaminergic neurotoxicity, Brain Res. 818 (1999) 575–578.

[24] B. Halliwell, J.M. Gutteridge, Lipid peroxidation, oxygen radicals, Cell Damage Antioxid. Ther. 23 (1984) 1396–1397.
[25] D.T. Dexter, C.J. Carter, F.R. Wells, Y. Javoy-Agid, A. Lees, P. Jenner, C.D. Marsden, Basal lipid peroxidation in substantia nigra is increased in Parkinson's disease, J. Neurochem. 52 (1989) 381–389.
[26] D.T. Dexter, F.R. Wells, A. Lees, Increased nigra iron content and alterations in other metal ions occurring in brain in Parkinson's disease, J. Neurochem. 52 (1989) 1830–1836.
[27] C.D. Smith, J.M. Carney, P.E. Starke-Reed, C.N. Oliver, E.R. Stadtman, R.A. Floyd, W.R. Markesbery, Excess brain protein oxidation and enzyme dysfunction in normal aging and Alzheimer disease, Proc. Natl. Acad. Sci. U. S. A. 88 (1991) 10540–10543.
[28] R.J. Ragusa, C.K. Chow, J.D. Porter, Oxidative stress as a potential pathogenic mechanism in an animal model of Duchenne muscular dystrophy, Neuromuscul. Disord. 7 (1997) 379–386.
[29] C.R. Cornett, W.R. Markesbery, W.D. Ehmann, Imbalances of the trace elements related to oxidative damage in Alzheimer disease brain, Neurotoxicology 19 (1998) 339–345.
[30] F. Facchinetti, V.L. Dawson, T.M. Dawson, Free radicals as mediators of neuronal injury, Cell Moi. Neurobiol. 18 (1998) 667–682.
[31] Y. Sagara, S. Tan, P. Maher, D. Schubert, Mechanisms of resistance to oxidative stress in Alzheimer's disease brain, Neurotoxicology 19 (1998) 339–345.
[32] S. Tan, M. Wood, P. Maher, Oxidative stress induces a form of programmed cell death with characteristics of both apoptosis and necrosis in neuronal cells, J. Neurochem. 71 (1995) 95–105.
[33] T.S. Kim, D.W. Jeong, B.Y. Yun, I.Y. Kim, Dysfunction of rat liver mitochondria by selenite: induction of mitochondrial permeability transition through thiol-oxidation, Biochem. Biophys. Res. Commun. 294 (2002) 1130–1137.
[34] S.L. Carlson, M.E. Parrish, J.E. Springer, K. Doty, L. Dossett, Acute inflammatory response in spinal cord following impact injury, Exp. Neurol. 151 (1998) 77–88.
[35] T.S. Lewis, P.S. Shapiro, N.G. Ahn, Signal transduction through MAP kinase cascades, Adv. Cancer Res. 74 (1998) 49–139.
[36] Z. Xia, M. Dickens, J. Raingeaud, R.J. Davix, M.E. Greenberg, Opposing effects of ERK and JNK-p38 MAP kinase on apoptosis, Science 270 (1995) 1326–1331.
[37] S. Nakahara, K. Yone, T. Sakou, S. Wada, T. Nagamine, T. Niiyama, H. Ichijo, Induction of apoptosis signal regulating kinase 1(ASK1) after spinal cord injury in rats: possible involvement of ASK1-JNK and -p38 pathway in neuronal apoptosis, J. Neuropathol. Exp. Neurol. 58 (1999) 442–450.
[38] H. Ozawa, S. Shioda, K. Dohi, H. Matsumoto, H. Mizyshima, C.J. Zhou, H. Funahashi, Y. Nakai, S. Nakajo, K. Matsumoto, Delayed neuronal cell death in the rat hippocampus is mediated by the mitogen -activated protein kinase signal transduction pathway, Neurosci. Lett. 262 (1999) 57–60.
[39] B. Sveneeon, P.A.B. Ekstrom, Mitogen activated protein (MAP) kinase activity is induced in adult mouse superior cervical ganglia during culturing, J. Neurosci. Res. 52 (1998) 453–457.
[40] C.N.G. Anderson, A.M. Tolkovsky, A role for MAPK/ERK in sympathetic neuron survival: protection against a p53-dependent, JNK-independent induction of apoptosis by cytosine arabinoside, J. Neurosci. 19 (1999) 664–673.
[41] M. Shamloo, A. Rytter, T. Wieloch, Activation of the extracellular signal-regulated protein kinase cascade in the hippocampal CA1 region in a rat model of global cerebral ischemic preconditioning, Neuroscience 93 (1999) 81–88.
[42] K.P. Sarker, K.K. Biswas, J.L. Rosales, K. Yamaji, T. Hanshiguchi, K.Y. Lee, I. Maruyama, Ebselen inhibits NO-induced apoptosis of differentiated PC12 cells via inhibition of ASK1-p38 MAPK-p53 and JNK signaling and activation of p44/42 MAPK and Bcl-2, J. Neurochem. 87 (6) (2003) 1345–1354.
[43] M.P. Scheid, J.R. Woodgett, Unraveling the activation mechanisms of protein kinase B/Akt, Exp. Neurol. 166 (2003) 115–126.
[44] D.P. Brazil, Z.Z. Yang, B.A. Hemmings, Advances in protein kinase B signaling: AKTion on multiple fronts, Trends Biochem. Sci. 29 (2004) 233–242.
[45] L.L. Jones, R.U. Margolis, M.H. Tuszynski, The chondroitin sulfate proteoglycans neurocan, brevican, phosphacan, and versican are differentially regulated following spinal cord injury, Exp. Neurol. 182 (2003) 399–411.
[46] M.J. Jurynec, C.P. Riley, D.K. Gupta, T.D. Nguyen, R.J. McKeon, C.R. Buck, TIGR is upregulated in the chronic glial scar in response to central nervous system injury and inhibits neurite outgrowth, Mol. Cell. Neurosci. 23 (2003) 69–80.